scientific reports

Check for updates

OPEN

Three-dimensional imaging reveals a hierarchical organisation of the myocardial mesh in mammalian hearts

Robert S. Stephenson[1], John Partridge[2], Jonathan C. Jarvis[3], Rajmund Mokso[4], Stephen Hall[5], Robert H. Anderson[6] & Peter Agger[7]✉

Despite intense investigation through centuries, there is still no scientific consensus on how to describe myocardial microarchitecture. This is mainly because the myocardium must be visualised in three dimensions, and with sufficiently high resolution to fully appreciate its complex nature. X-ray microtomography allows for exactly such visualisation. Using this technique, we herein provide a description of the ventricular mural architecture in a wide range of mammals. Myocardial biopsies from the left ventricle of a human, pig, rabbit, giraffe, elephant, and sei whale were imaged using X-ray microtomography after iodine staining. Aggregations of cardiomyocytes were segmented and visualised in three dimensions, permitting accurate assessment of their shape and orientation. It was possible to segment individual components of the overall mesh using the three-dimensional images in all the studied species. The myocardium is most accurately described as a complex hierarchical meshwork, with the cardiomyocyte as the smallest working unit. The cardiomyocytes are bound together by endomysium to form aggregates, which are themselves compartmented by perimysium. A high degree of variation in the shape of aggregation was found within each biopsy, but, most remarkably, significant differences were observed between species. Some bundles of aggregated cardiomyocytes stand out from the adjacent myocardium within the mesh due to a clear change in their orientation. We provide evidence that the mammalian ventricular myocardium is a complex meshwork of cardiomyocytes. This mesh, although continuous along its direction of contraction, is separated by perimysial clefts into aggregated entities most appropriately described as aggregates. When comparing between species, there is remarkable heterogeneity in this anatomical appearance. We found no evidence of the myocardium being ordered into a large individual band as previously described elsewhere.

Keywords Myocardial architecture, Myocardial aggregations, Anatomy, Myocardium

The function of any dynamic organ reflects its anatomy and hence clinical cardiologists assess the condition and performance of the heart by both anatomical and physiological measures. Some of these, however, depend on morphological presumptions that remain to be substantiated[1]. A good example of this is the presence, within the ventricular walls, of cardiomyocytes whose orientation is not strictly parallel to either the endocardial or epicardial surfaces. Some researchers consider this property as an important structural and functional feature[2,3], while others do not include it in their descriptions[4]. Another presumption is that cardiomyocytes are aggregated into secondary groups, or units, which have functional significance. There is an overall agreement that the cardiomyocytes are, indeed, grouped together by the endomysium of the fibrous matrix, but the names used for describing these groupings are far from uniform. Terms used include sheets[5], sheetlets[6], units[7], or, simply, as we prefer, aggregates[8]. This lack of consensus is caused by an absence of knowledge of the microanatomical nature of myocytic aggregation. This is in spite of the rising agreement that changes in the orientation of the

[1]Institute of Clinical Sciences, University of Birmingham, Birmingham, UK. [2]Retired From Eurobodalla Unit, Rural Clinical School of the ANU College of Medicine, Biology & Environment, Batemans Bay, NSW, Australia. [3]School of Sport and Exercise Sciences, Liverpool John Moores University, Liverpool, UK. [4]Department of Physics, Technical University of Denmark, Copenhagen, Denmark. [5]Division of Solid Mechanics, Lund University, Lund, Sweden. [6]Biosciences Institute, Newcastle University, Newcastle-Upon-Tyne, UK. [7]Comparative Medicine Lab, Department of Clinical Medicine, Aarhus University, Aarhus, Denmark. ✉email: peter.agger@clin.au.dk

cardiomyocytes are of paramount importance in the assessment of cardiac performance in both health and disease. Recent studies conducted by ourselves and others suggest that changes in orientation of the alleged subunits are the main driving force behind normal cardiac function[6,8]. In turn, it is anticipated that the orientation of the units, whatever their extent, is altered in different disease states[6,7,9]. From this, it follows that an understanding of their anatomical appearance, and subsequently their function in the heart, is imperative.

To date, the units are often described as flattened structures, which are presumed to assume the shape of a square or rectangle. This is probably a considerable over-simplification of the true morphology[1]. Most images available in the literature have been generated using electron-microscopy or histology. They show mainly cross-sections of the entities in question[5,6,10], and only a few studies show complete segmentation of groupings of cardiomyocytes, even then without further analyses or description[2]. The concept of the individual cardiomyocytes being aggregated into planar substructures within the myocardium originates from the works of LeGrice and colleagues[5,11,12]. They coined the term 'sheets' to describe the structure, with this terminology adopted by many groups. They argued, nonetheless, that '…the ventricular myocardium is not a uniformly branching continuum, but a laminar hierarchy…'[11]. The challenge that remains is that LeGrice and his colleagues, and many groups after them, ourselves included, have made inferences on the function of the proposed sheets, but with only limited knowledge of their anatomical extent or shape. This leaves a significant risk of misinterpretation. Thus, despite being a subject of intense investigation for several centuries, the architecture of the myocardium is still not completely understood. One school of thought continues to maintain that, because of the alignment of the chains of cardiomyocytes, it is possible to unwrap the ventricular cone in the form of a continuous helical band[13]. This notion originated from the studies of Francisco Torrent-Guasp[14]. Although compelling evidence has been provided to reveal the falsity of the concept by both anatomical[15–17] and physiological means[18], the concept retains its proponents in the scientific community[19,20]. Another school, endorsing the extensive account provided by Streeter following extensive histological investigations[21], argues that the cardiomyocytes are aggregated together to form a three-dimensional continuum, albeit with heterogeneous arrangement of sub-structures to produce a meshwork[22].

The problem thus far in arbitrating between these anatomical models, and hence the major obstacle to comprehensive understanding, has been the lack of a technique that provides sufficient resolution to identify the individual cardiomyocytes themselves, while at the same time permitting three-dimensional reconstruction of the manner of their aggregation. The development of X-ray microtomography now provides an opportunity to bridge this gap[23]. The aim of our present study was, therefore, to record and describe the myocardial mural architecture in several species using high-resolution X-ray tomography.

Materials and methods

We examined six transmural myocardial biopsies, one from each of the following mammalian species: human (*Homo sapiens*) originating from the dept. of forensics, Aarhus University. The sei whale (*Balaenoptera borealis*) from a whale stranding in Denmark. The giraffe (*Giraffa camelopardalis*) from Ree Park, Ebeltoft, Denmark. The Asian elephant (*Elephas maximus*) from Copenhagen Zoo, Denmark. The domestic pig (*Sus scrofa domesticus*) from the Aarhus Heart Archive, Denmark. And the rabbit (*Oryctolagus cuniculus*), specimen from Liverpool John Moores University, UK. All biopsies were taken from the left ventricle at the level of its equator. Thus, we could compare our own species with a broad range of other mammals with extremes of size and blood pressure, including some experimental animals. Human tissue samples used in this study were anonymised residual diagnostic specimens while animal biopsies were obtained post-mortem and collected in accordance with the EU Animal By-Products Regulation (EC No. 1069/2009), thus all specimens were collected with appropriate permissions according to Danish legislation.

Contrast enhanced X-ray microtomography

X-ray microtomography scanning was carried out using the Zeiss XRadia Versa XRM520 at the 4D Imaging Lab at Lund University, and the Nikon Xtek High Flux Bay system at the Henry Moseley X-ray Imaging Facility, University of Manchester, as previously described by Stephenson et al.,[24]. Prior to scanning, samples were immersed in potassium iodide with concentration and incubation times dependent on the sample size (see Supplemental Table S1), based on previous experience[24]. Samples were cleared of fixative and excess contrast medium by washing in distilled water before being immobilised in a plastic holder. Scans were acquired with X-ray tube voltages ranging from 60–224 kV. Scans were performed through 360 degrees sample rotation, with between 1601 and 3142 projections. A tungsten target was used for all scans, with a manufacturer supplied Le3 source filter for the Versa scans and a 3 mm aluminium filter used for the High Flux Bay scans. Single scan times ranged from 50 to 265 min. The projection data were reconstructed using filtered back-projection in the proprietary software of each system, resulting in tomographic image data with isotropic voxel volumes ranging from 1.63–39.33 μm^3 (see Supplemental Table S1 for further details).

Identifying and segmenting the aggregated cardiomyocytes

We used several structural definitions to assess the aggregation of the individual cardiomyocytes. We defined the long axis, or length, of a given segmented portion or component of the myocardial mesh as the prevailing long axis orientation of the individual myocyte chains housed within it. Consequently, the short axis was defined according to the short axis of the individual myocytes. The components were identified as being contiguous, high attenuating structures surrounded by low attenuating perimysial space. As such, they proved to be part of a global three-dimensional branching network. For the purpose of comparison between the species, we chose to segment components of the mesh according to the pattern of their branching. Segmentation of the voxels within each component of the mesh was performed using a semi-automated process, combining the use of the 'paintbrush tool' and interpolation function in Amira v5.3.3 (Thermo Fisher Scientific), as described

previously[24]. Segmentation was performed initially in the short axis plane, including branches to adjacent components in the segmentation (Fig. 1). Segmentation in this fashion was continued in distal and proximal directions along the long axis until the component of interest branched to a larger component, or else it ceased to exist. Some segmented entities split into multiple branches. In these instances, the largest branch was included in the segmentation. Segmentation was stopped at the point where the component joined with, or formed, a new larger component, as this was deemed the commencement of a new component within the overall mesh. Segmentation was then completed using orthogonal views. In this way, the segmented entity could be identified simultaneously in its short, long, and transverse axes, ensuring that only voxels were included, which were a part of the entity itself, or its major branches.

Quantification of segmented structures

The orientation of each segmented entity was quantified using a custom-made Excel macro (Microsoft Corporation, 2018) as outlined in Fig. 2. For each component, the coordinates of three points of interest were extracted using Amira (version 5.3.3). Of these points, two were aligned so as to form a straight line that coincided with the orientation of the chains of cardiomyocytes within the component. From this line, the orientation of the identified cardiomyocytes was calculated in terms of their helical and intrusion angles. Because the cardiomyocytes are appreciated, in mathematical terms, as two-dimensional lines in a three-dimensional space,

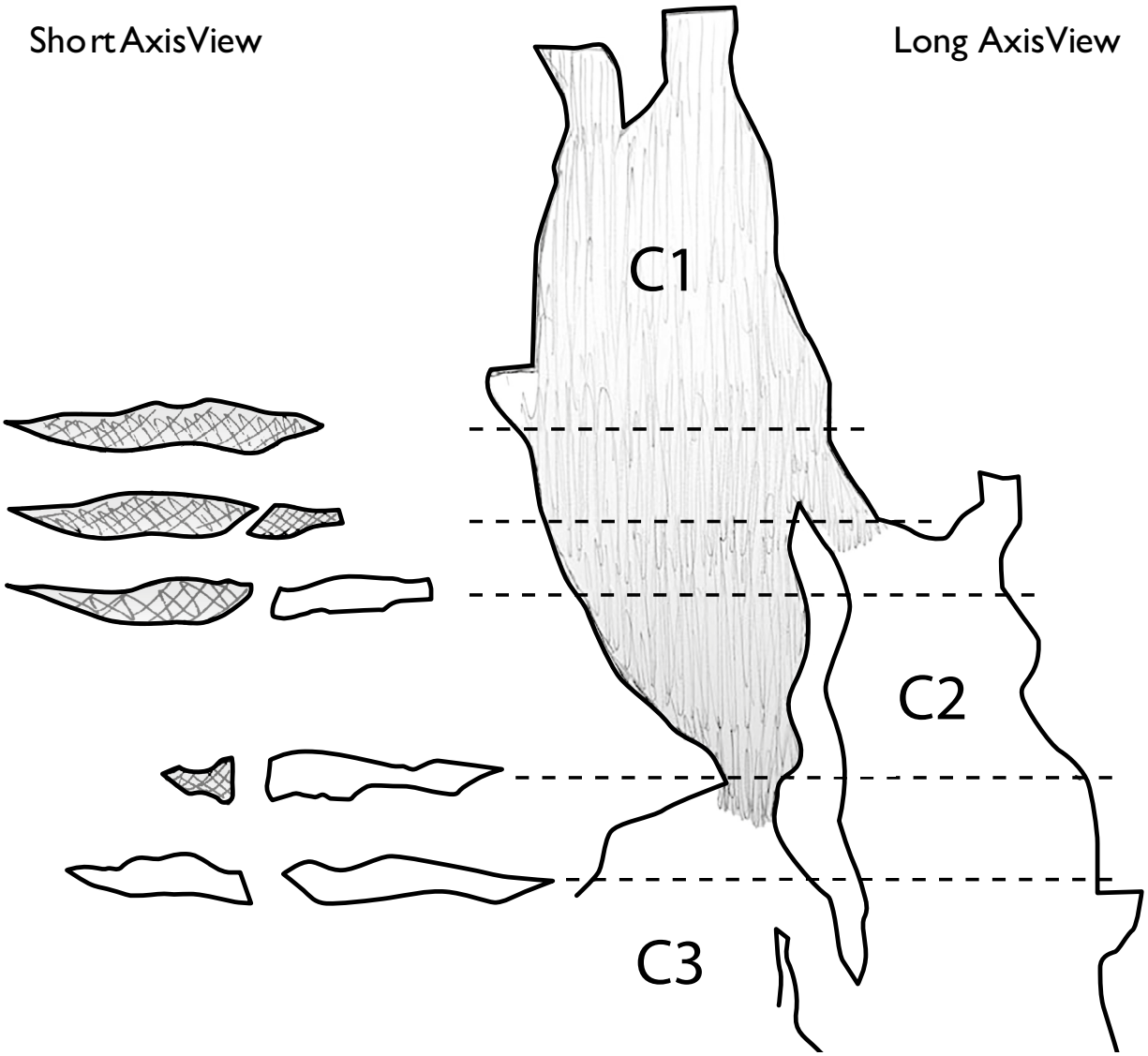

Fig. 1. Components of the myocardial mesh were segmented according to the pattern of their branching. Segmentation was performed initially in the component short axis plane (left panels), with branches to adjacent components (C2 and 3) of the mesh originating from the component of interest (C1) included in the segmentation. The adjoining components themselves were not included. In case of splitting into multiple branches, only the largest branch was included in the segmented entity. When any branch joined with, or formed, a new larger component of the mesh, segmentation ceased.

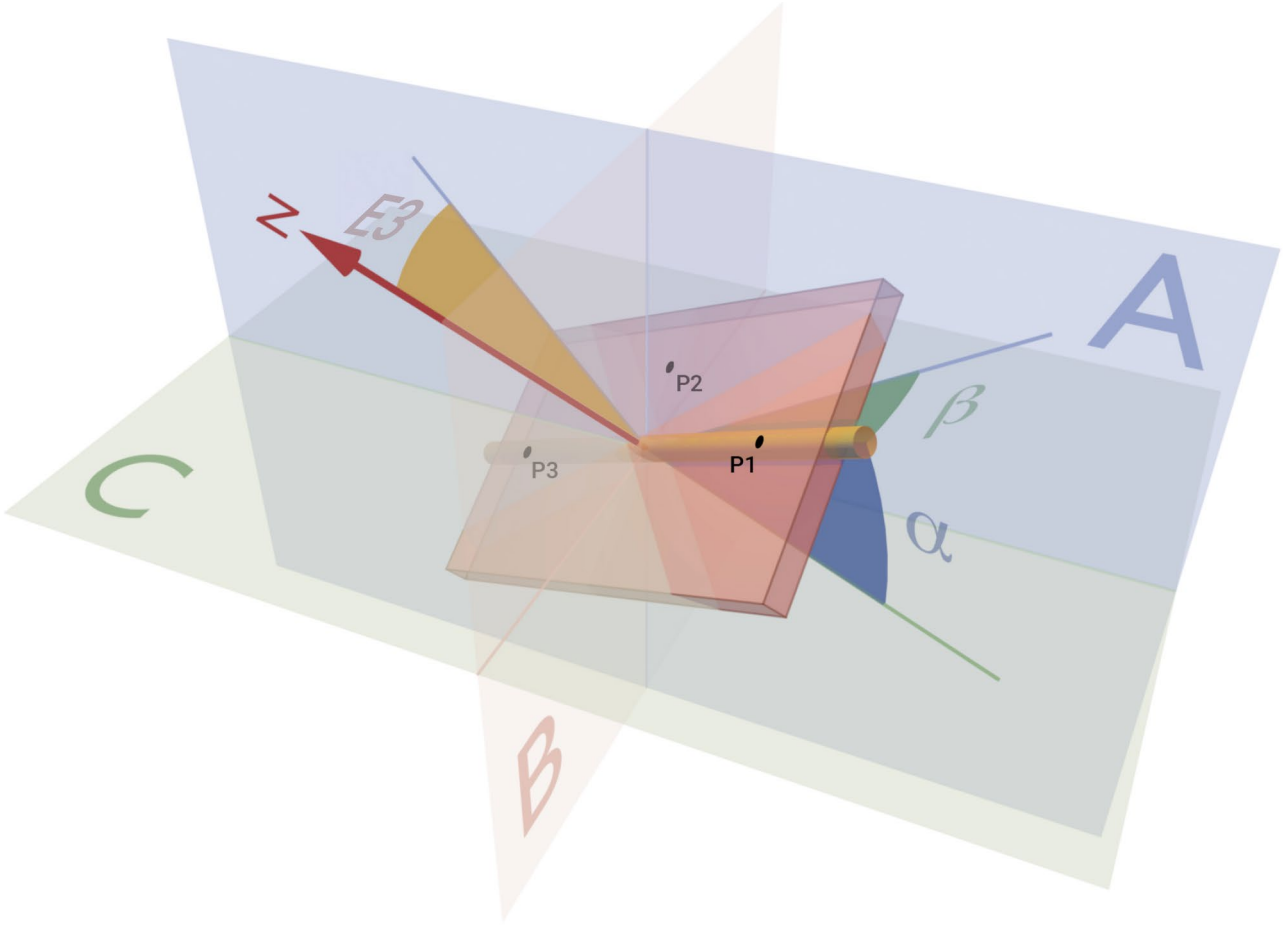

Fig. 2. Schematic of angles used to quantify cardiomyocyte and component orientation. A chain of cardiomyocytes (yellow rod) embedded in a component (red box) is treated as a line in three-dimensional space. Its orientation is defined by the helical angle (α), the angle between the chain and the circumferential–radial plane (plane C), and the intrusion angle (β), the angle between the chain and the longitudinal–circumferential plane (plane A). The component is treated as a plane, and its orientation is defined as the angle between the component plane, given by its normal vector (N), and the longitudinal–circumferential (epicardial tangential) plane A, the so-called E3-angle. The component normal vector is calculated from three surface points (P1–P3) where P1 and P3 are aligned with the cardiomyocyte chain, while P2 is a non-collinear point on the component surface.

it is not possible to calculate the overall orientation of the three-dimensional segmented components from the known helical and intrusion angles. To circumvent this problem, we placed a third point, out of line with first two, but still in the plane of the component. Taken together, these three points provide a plane. This plane coincides with the plane of the entity from which the orientation of the segmented entity itself can be determined in terms of its E3-angle, also often referred to as the sheet angle. All three angles were measured relative to the epicardial surface of the biopsies. The interested reader can find a detailed mathematical description of all angles in our previous publication[1].

Results

Aggregation of the individual cardiomyocytes

In all biopsies, the high-resolution imaging revealed a complex three-dimensional meshwork of aggregated individual cardiomyocytes. Within the mesh, the aggregated chains of individual cardiomyocytes showed markedly anisotropic orientations. Compartmentalisation of the myocardium was found in all six investigated species (Fig. 3). When assessed in the short-axis and radial planes, the aggregated chains ran in numerous directions, both in and out of plane. A clear helical orientation, nonetheless, can be observed in the epicardial tangential plane, as shown in Supplemental Video 1. Within the mesh thus formed, we were able to identify groups of cardiomyocytes with near-identical orientation, aggregated together by endomysial connective tissue. For our ongoing descriptions, we have chosen to refer to these groupings simply as an aggregate, thereby avoiding any morphological reference. The differences in the architecture of the supporting fibrous matrix, along with differences of texture of the chains within the produced images, meant that the chains are best discerned in the radial plane. This corresponds approximately to the short-axis of the aggregated cardiomyocytes themselves.

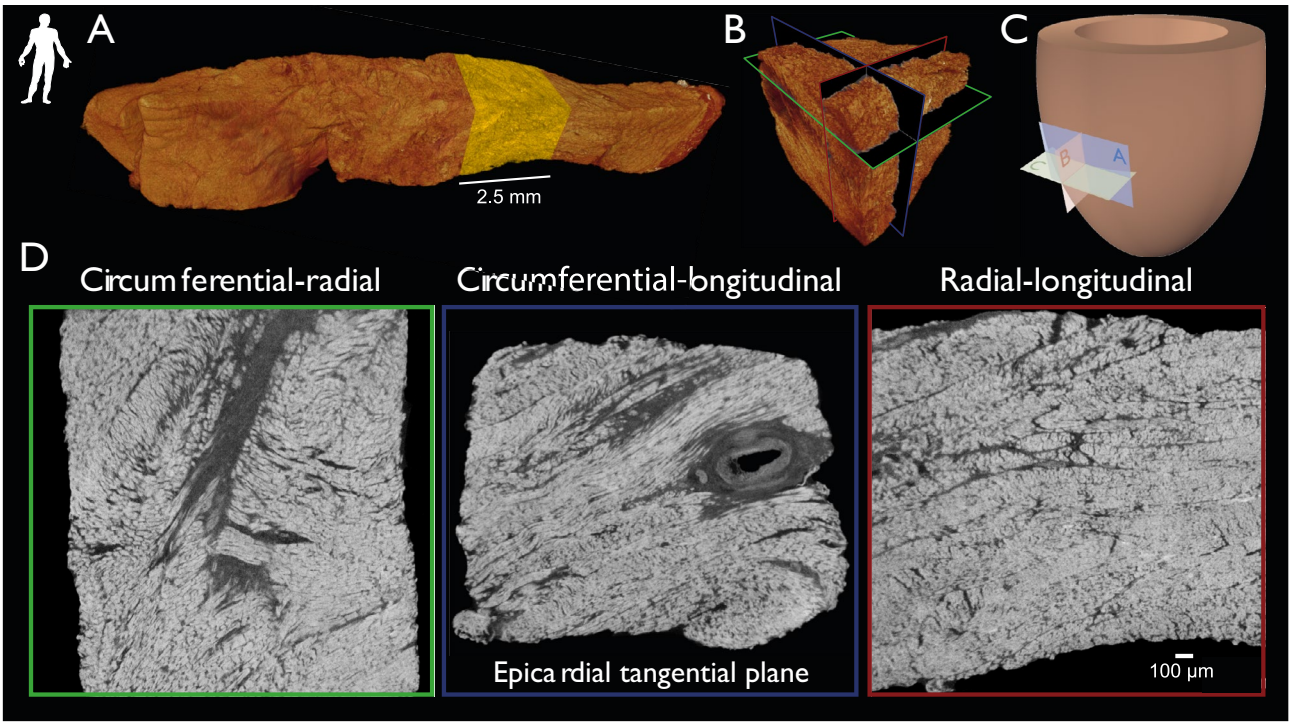

Fig. 3. Global reference planes: Panel (**A**) High-resolution X-ray microtomography of a transmural human heart biopsy. A subset (yellow) is selected for virtual orthogonal transection (Panel **B**). Panel (**C**) The global orthogonal planes are shown with reference to the left ventricular myocardium. Resulting orthogonal views are shown below in Panel (**D**). Each orientation is colour-coded as green for the circumferential-radial plane, blue for the circumferential-longitudinal plane, often referred to as the epicardial tangential plane, and red for the radial-longitudinal plane. The colour-coding is maintained for the remainder of the figures.

The compartmentalisation is observed in all species, with the aggregates themselves separated by the perimysial clefts within the extracellular matrix. The clefts provide potential planes of slippage between the aggregated entities (Fig. 4 and supp. Video 1).

Three-dimensional morphology of the aggregated cardiomyocytes

As described above, we chose to recognise the segmented components according to the extent of their branching within the overall three-dimensional arrangement of the ventricular walls. Assessing the biopsies from the human hearts by means of volume rendering permitted recognition of the individual cardiomyocytes within their chains. The chains themselves run in the long axis of the component of the aggregated mesh, branching to join adjacent parts of the mesh (Fig. 5A). Sectioning in the radial plane shows the short axis of the segmented component of the aggregated mesh (Fig. 5B). Having segmented the entity in the fashion defined, it is possible to assess its orientation in the three orthogonal planes (Fig. 5C). We found significant morphological heterogeneity of such aggregated entities, both within the individual species and across the species investigated (Fig. 6). The shapes varied from being flat in the giraffe and rabbit, to having a more tubular appearance in the elephant and whale. Within all species, the aggregated entities, as segmented, themselves displayed a wide variation in size in all dimensions. In the light of the marked intra- and interspecies variation in both dimensions and overall morphology, an attempt to quantify the precise dimensions of the aggregates makes little sense. Even the shape of adjacent aggregated entities, moreover, was seen to change markedly as they were traced either transmurally (Fig. 6), or in the long axis of the left ventricle (Fig. 7).

Three-dimensional orientation of the myocardial components

By following the extent of the components, we were able to trace adjacent segmented entities in transmural fashion (Fig. 6). This revealed the anticipated transition in helical angulation from -90° in the subepicardium to + 90° in the subendocardium (Fig. 6; top panel). While generally maintaining their helical angulation, parts of the aggregated mesh showed marked changes in both intrusion and E3 angulation. Tracing of such changes in the longitudinal-radial plane in the human left ventricle is shown in Figs. 7 and 8. Aggregated entities not directly connected to one another are shown in Fig. 7. In Fig. 8, we show segmented aggregations within the three-dimensional mesh interconnected by direct branching. Marked local variations were found in both settings when using all conventional measures of orientation (Figs. 7 and 8). Differences in both helical and intrusion angles of adjacent aggregates amount to more than 45° in some cases. Although we have illustrated the changes only in the subepicardium, this heterogeneity was present across the thickness of the wall in all species investigated.

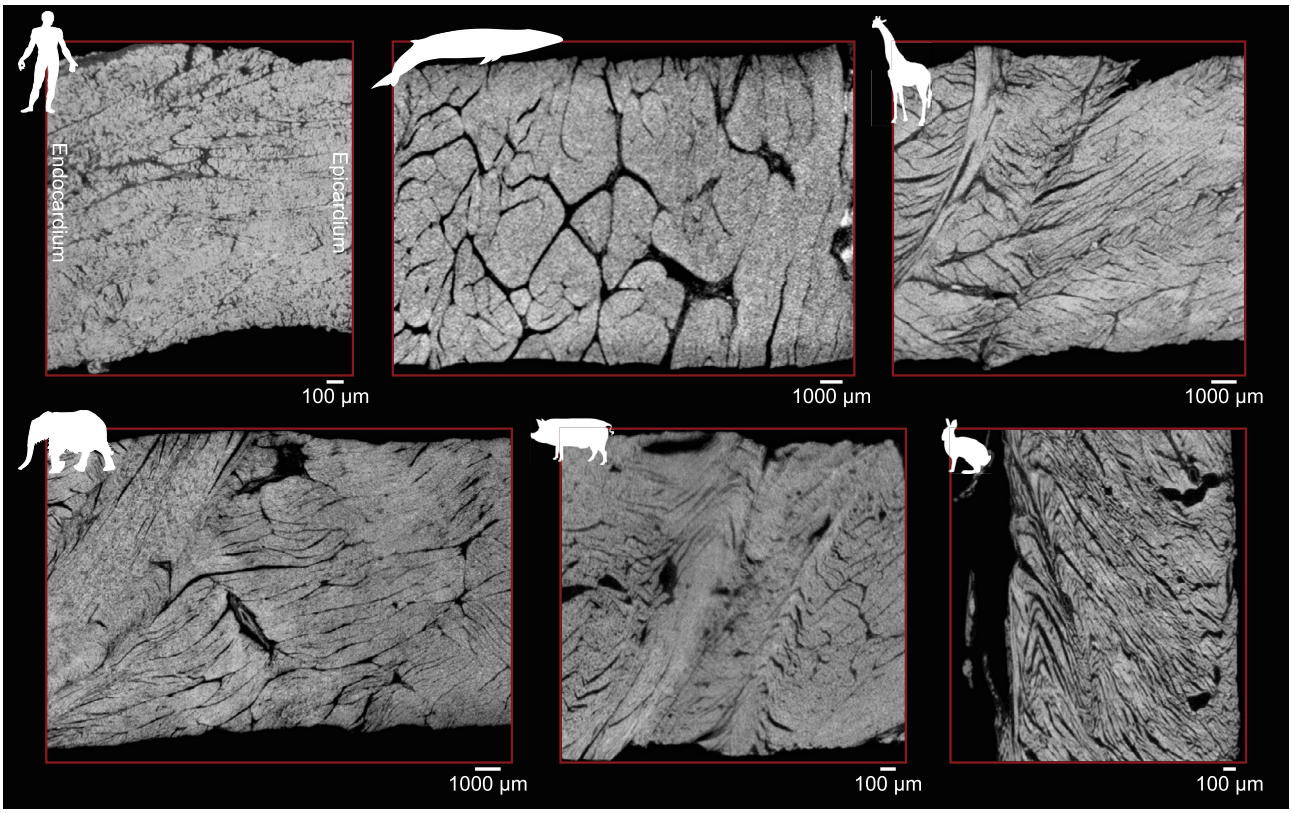

Fig. 4. X-ray microtomography of the subepicardium in different mammalian species. All tomograms are reconstructed in the radial-longitudinal plane, with the epicardial direction towards the right, and the endocardium towards the left. The human (top left), the Sei Whale (Balaenoptera borealis, top center), the giraffe (Giraffa camelopardalis, top right), the asian elephant (Elephas maximus, bottom left), the domestic pig (Sus scrofa domesticus, bottom center), and the rabbit (Oryctolagus cuniculus, bottom right) are shown.

Higher order aggregation within the three-dimensional mesh

On the basis of the markedly different orientations of some segmented entities compared with those making up their surrounding myocardium, we were able to observe a higher order of aggregation within the three-dimensional mesh revealed by the tomographic imaging (Fig. 9). The segmentation revealing this higher order aggregation was performed in the same manner as outlined above when segmenting the regular entities. Segmentation was performed initially in the short axis plane of the higher order entity, with clear differences in orientation between the entity and the surrounding myocardium demarcating its lateral extremity. Such segmentation was again continued in distal and proximal directions until it was no longer possible to identify the higher order aggregation within the overall three-dimensional mesh.

The higher order aggregations were found in all investigated species (Fig. 9). They were all constructed from the initially identified individual aggregations, which had themselves been aggregated into thicker bundles. These bundles could be identified as running almost independently of the surrounding mesh with the chains of cardiomyocytes aggregated within the bundles orientated at marked angulations to those making up the larger part of the adjacent mesh (Fig. 9, left hand panels and supp. Video 1). These seemingly independent bundles, nonetheless, remained an integrated part of the overall three-dimensional mesh, forming hinge-like connections with adjacent aggregated entities, and displaying rapid transitions of more than 45° in their orientations. When segmented and rendered in three dimensions, the identified bundles could be seen to be of considerable size, and to extend with a significant transmural angulation (Fig. 9, right hand panels). A pronounced feature of the bundles deviating from the tangential plane is that they tend to twist and bend as they progress through the myocardium, sometimes just slightly, sometimes markedly. This means that the orientation of the middle parts of the bundles are not necessarily the same as the orientation at their ends. Because of this, we have not attempted to quantify their overall orientation, as it would be difficult to apply any interpretation to a parameter that is not constant within it.

Discussion

Our data show that, in all the investigated species, the ventricular walls are made up of a continuous three-dimensional mesh of aggregated individual cardiomyocytes. Within the mesh, the individual cardiomyocytes are grouped together by the endomysium of the fibrous matrix. The aggregated entities thus formed are then separated by the perimysial spaces, while still interconnected by their branching. The entities identified as making

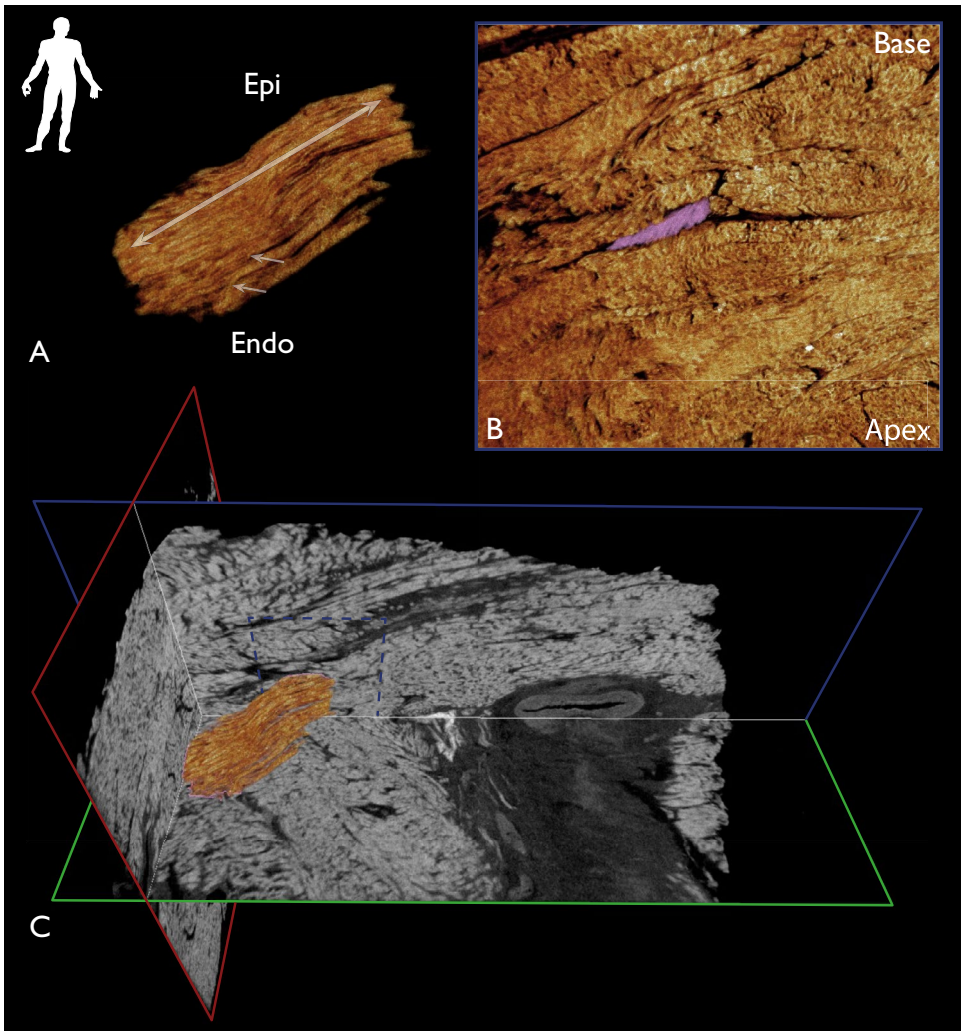

Fig. 5. The images show, in panel (**A**), an example of the manner of aggregation of cardiomyocytes found in the human heart. It is an easy matter to visualise the chains of individual myocytes aggregated together, and to discern their long axis, as shown by the double-headed arrow. The branching components, signifying the margins of the segmented entity, are shown by single-headed arrows. Panel (**B**) shows the location of the aggregated entity, outlined in pink, as viewed in the radial plane. Panel (**C**) shows a three-dimensional rendering of the entity as located in the overall transmural section of the biopsy. Note the thin pink outline where the entity transects the orthogonal tomograms.

up the mesh vary tremendously in terms of their shape, size, and orientation, both within the individual hearts and between the investigated species. These components are predominantly of a flattened nature, although the degree of flatness itself varies, especially between species. Because of this morphological variation, we do not find it meaningful to name these structures by reference to their anatomical shape. Thus, we consider names such as sheet or sheetlet to be inappropriate as they indicate the structures to be flattened. We suggest, at present, it is appropriate simply to describe these structures as aggregates and will do so in the following. To the best of our knowledge, we provide the most comprehensive three-dimensional reconstruction of the aggregates currently available. The aggregates are sufficiently large to form the basis of the "grain" seen in gross anatomical dissections[25]. Thus, it is the extent of aggregation within the mesh that provides the "missing link" in the scale of myocardial construction. Previous studies have described two distinct populations of aggregates with opposite sign[10]. We confirm the existence of aggregates with opposite signs (Figs. 7 and 8), but are unable to elucidate their distribution as this would require segmentation of numerous aggregates.

Surprisingly, some aggregates within the mesh, as we have segmented them, are themselves grouped into larger entities of higher order. These larger entities are recognisable within the mesh by their differing orientation, yet remain part of it. As far as we are aware, this finding is previously undescribed. These entities are relatively large, as they tend to scale with the size of the heart. As emphasised, they yet continue to branch within the surrounding overall mesh. We have chosen to describe them as bundles, as this is how they appear when segmented within the mesh. Taken together, both the aggregated long chains of cardiomyocytes, and the bundles of higher order, as thus defined, branch extensively. They are parts of the overall myocardial mesh, and

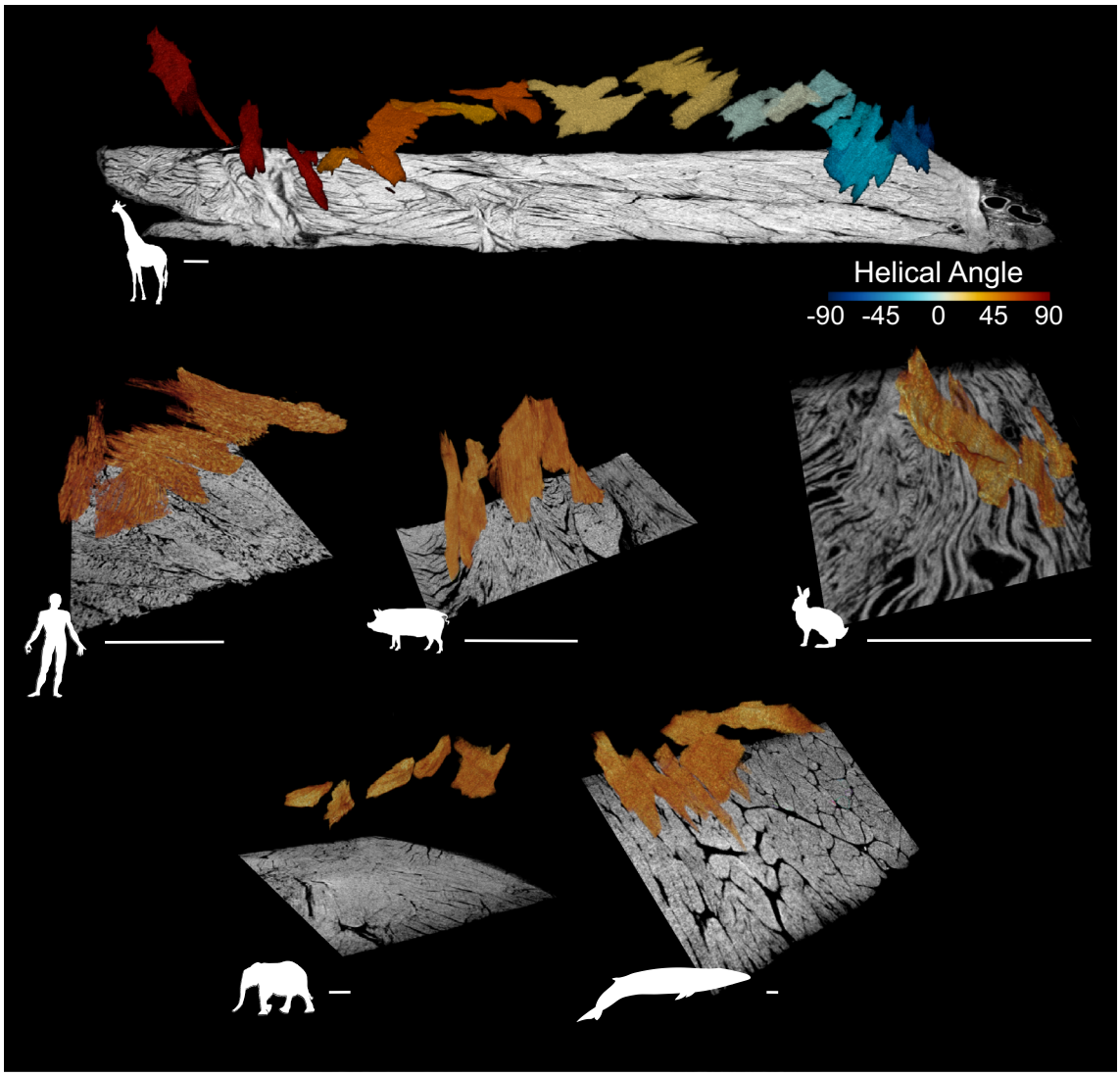

Fig. 6. The panels show the variation in the orientation of the aggregated entities as viewed across the transmural extent of the biopsies. The top panel shows a complete transmural biopsy from a giraffe. The colour-coding shows the helical angulation of the myocytic chains. The remaining panels display segmented aggregates from the subepicardial regions of the remaining species, which are shown by the insets. All scale bars are 1 mm.

not "stand-alone" entities. Likewise, considering their heterogeneity, it is not meaningful to attempt accurately to quantify their dimensions. The overall arrangement of a meshwork was found to extend through the entirety of our biopsies. We presume it extends in comparable fashion throughout the entire ventricular myocardium. Given that we are studying biopsies, however, we are unable to confirm this. Investigation of the entirety of the heart, and the global architecture of the entire ventricular cone, are important matters for future study. This will require scanning of the entire organ with a resolution comparable to that we have presented here. This is now possible with the Hip-CT technology offered by synchrotron X-ray facilities[26]. Our own study, nonetheless, has shown that significant insights can be gained with biopsies and more commonly available laboratory X-ray microtomography equipment.

The hierarchy of the heart

It has been stated that four to five individual cardiomyocytes are aggregated together to produce "sheets"[27]. This is a gross overinterpretation of the initial work of LeGrice and colleagues[11], who introduced the notion of the myocardial aggregate. LeGrice and his associates, nonetheless, emphasised that the myocardium is arranged in a heterogenous laminar hierarchy, with aggregates varying in thickness from one to 12 myocytes. While this is true for the most part, our results show an even higher degree of variation and heterogeneity than originally identified by LeGrice and his colleagues. The previous studies evaluating myocardial architecture, including that of LeGrice and co-workers, furthermore, were conducted using a range of different animal species, from pigs, through dogs, to rodents[8,11,27]. The marked interspecies variation we have now documented highlights the

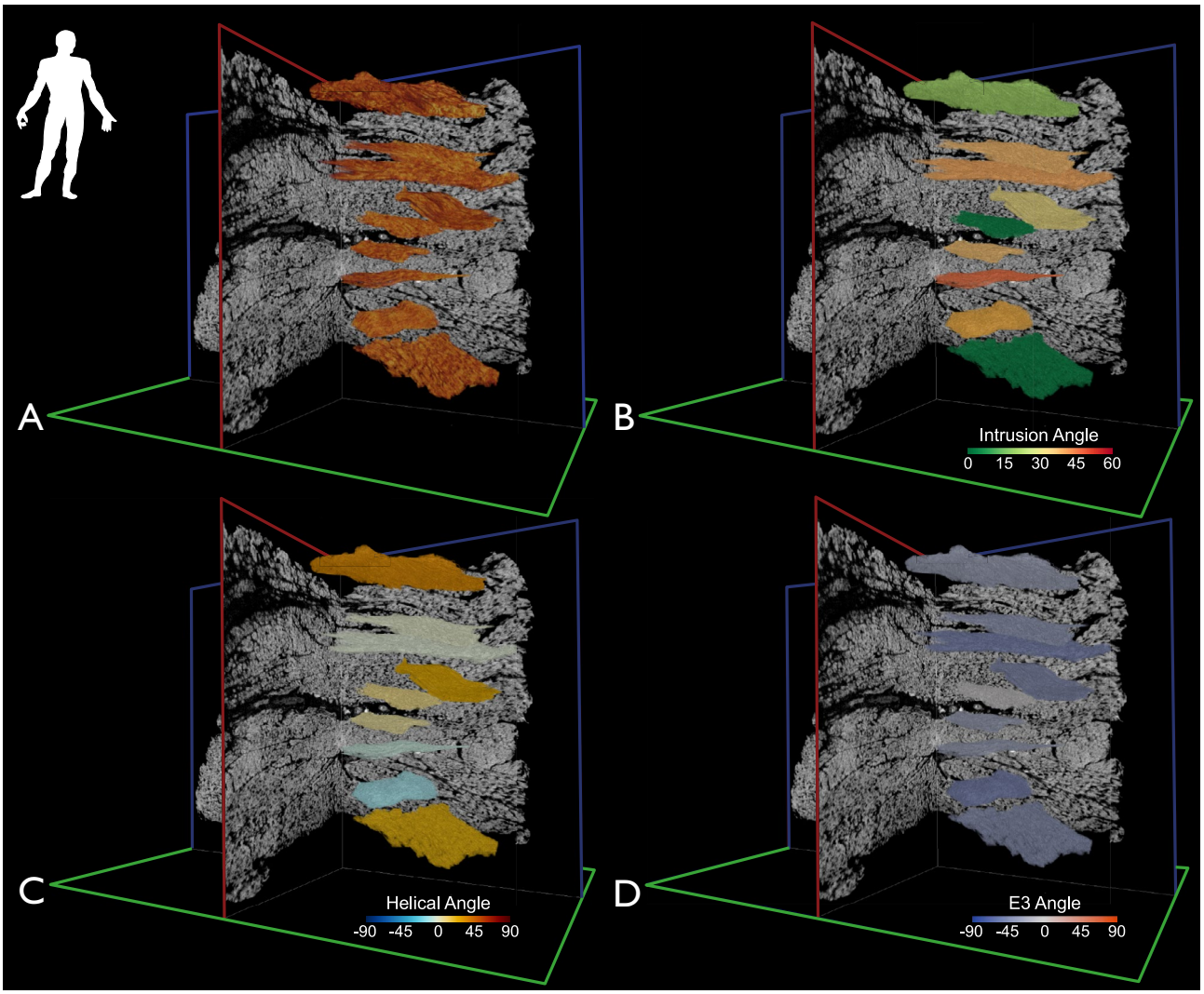

Fig. 7. The panels show the local variation as observed in the longitudinal axis apex to base direction for different aggregated entities in the human heart. All entities are located at the same radial level. Panel (**A**) shows the raw three-dimensional segmentation, along with an opacity-based colour map. Panel (**B**) then shows the same renderings colour-coded according to their transmural orientation as assessed based on their angle of intrusion. In panel (**C**), the aggregated entities have been colour-coded to show their helical orientation, while in panel (**D**) they are colour-coded according to their orientation as assessed based on the calculated E3 angle.

challenge of using these analogue species to draw conclusions on the structure of the human heart, a process which is far from infrequent. The different species studied, nonetheless, do share one common trait: the presence of an obvious myocardial architectural hierarchy. No obvious qualitative species differences were observed in the frequency of branching and merging within the myocardial mesh, although a rigorous comparison would require automated large-scale segmentation. Our current findings confirm that the myocytes within the ventricular walls form a complex continuum, previously referred to as the cardiac meshwork. Within this meshwork, the smallest working unit is the cardiomyocyte. The contraction of the myocyte, of course, is facilitated by its constituent myofibrils. But, since the myofibrils are all oriented predominantly within the long axis of the myocyte, it seems reasonable to continue to argue that the smallest functional entity within the heart is the cardiomyocyte itself. The individual cardiomyocytes are then aggregated together within the supporting endomysial part of the fibrous matrix. It follows that the connective tissue must also play an important supportive, albeit passive, role in cardiac deformation. The aggregates that we have segmented are separated by spaces, or clefts. These clefts contain the loose perimysial part of the fibrous matrix, along with blood vessels and nerves[28]. The surprising finding from our study was that, on occasion, the cardiomyocytes were aggregated together into much larger bundles. These larger entities are almost macroscopic. On occasion, they also show an obvious transmural angle. It is possible the presence of these transmural entities within the overall three-dimensional mesh (Fig. 9) is the substrate for myocardial antagonism, providing structural validation of the site of the auxotonic, as opposed to unloading, forces recorded using force probes[29].

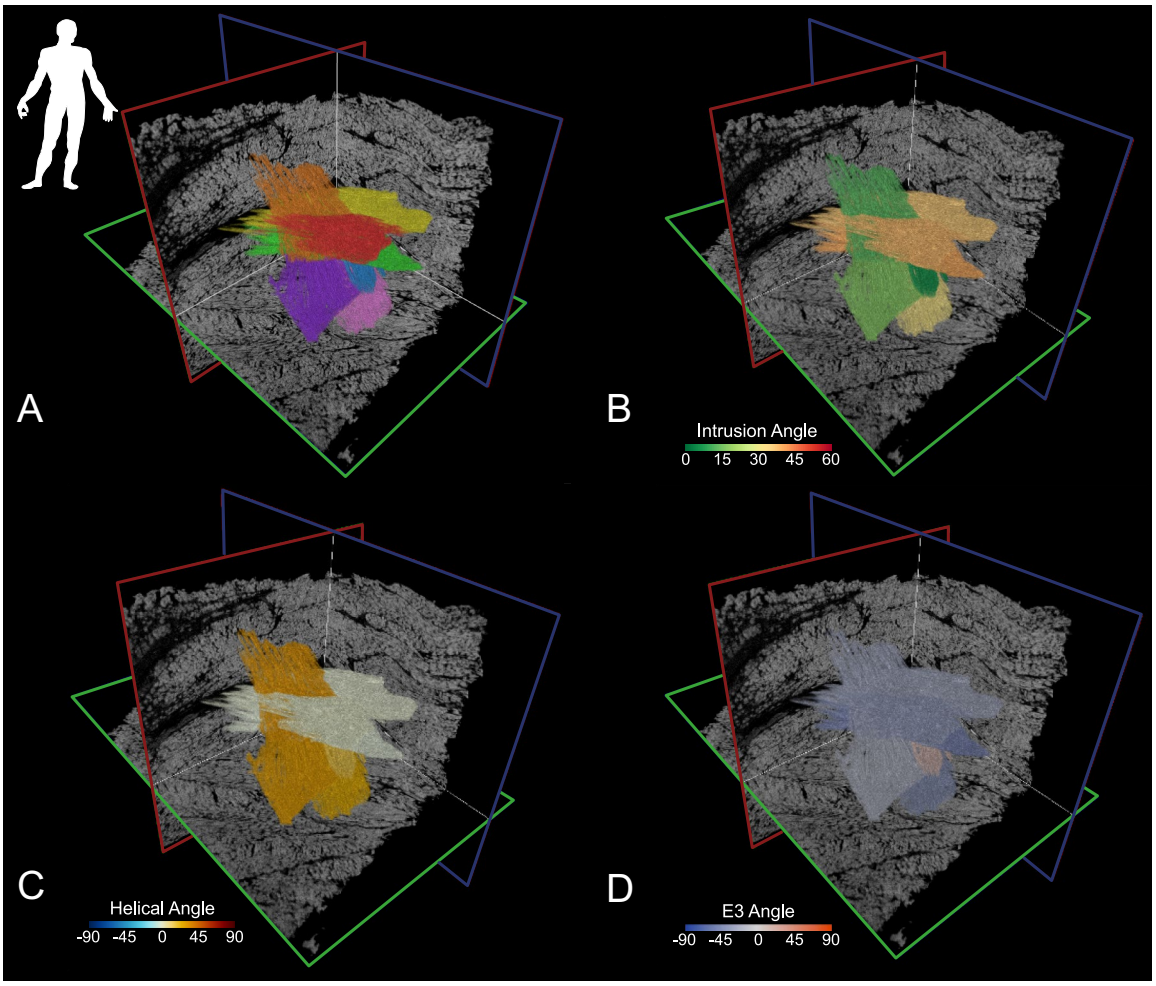

Fig. 8. The panels show the marked variation in the orientation of the aggregated entities in the human heart, which are directly linked by their branching. In the top left panel, the individual aggregates are coloured randomly, allowing the viewer to appreciate the place of the entities within the three-dimensional mesh. In panel (**B**), the same aggregates are colour-coded to show their angle of intrusion, with the colour-coding in Panel (**C**) showing the helical angulation, and panel (**D**) showing the E3-angle.

Some reports have depicted the myocardium as a layered structure, akin to the layers of an onion, with the layers made up of cardiomyocytes with a strictly surface-parallel orientation[30]. Our investigation shows no evidence supporting such layering. Also, we found nothing in our segmentations to support the notion that the ventricular cone could be unwrapped as an ordered and solitary helical ventricular myocardial band[14]. An alleged bi-layered structure for the ventricular wall has subsequently been suggested to provide proof of the alleged myocardial band[31]. This arrangement was nowhere to be found in our full thickness biopsies, which were taken from all six species from various parts of the left ventricular cone, including the ventricular septum. Adjacent aggregated entities showed marked differences and abrupt changes in all orientations. These changes, however, were observed only at the level of the entities themselves. They do not seem to represent a global phenomenon, as has been argued by others. Our findings, therefore, reinforce the idea of the myocardium as a complex cardiac mesh. They invite discussion in particular regarding the smooth transitions in helical angulation reported in the literature when using low resolution imaging, such as in diffusion tensor imaging[6,9].

Functional implications

Thanks to our state-of-the-art, high-resolution microtomographic imaging, we have now provided an overview of the ventricular mural architecture. As outlined, the individual cardiomyocytes are grouped into aggregated entities within a three-dimensional mesh, with some of the entities further aggregated into bundles. Within the aggregated entities, as segmented, the cardiomyocytes attain a common orientation, which provides the "grain" as observed by those dissecting the ventricular cone (See Fig. 5). Neither a segmented aggregate, nor a bundle of aggregates, can mimic a fascicle of skeletal muscle. This is because they cannot form a long straight line. In part, this is because the ventricular wall is curved, but more so because the aggregated entities do not have a tendinous origin and insertion. Instead, the aggregates and bundles form straight lines over short-to-medium distances. They branch and merge with their neighbours, with their orientation likely mediated by local loading conditions.

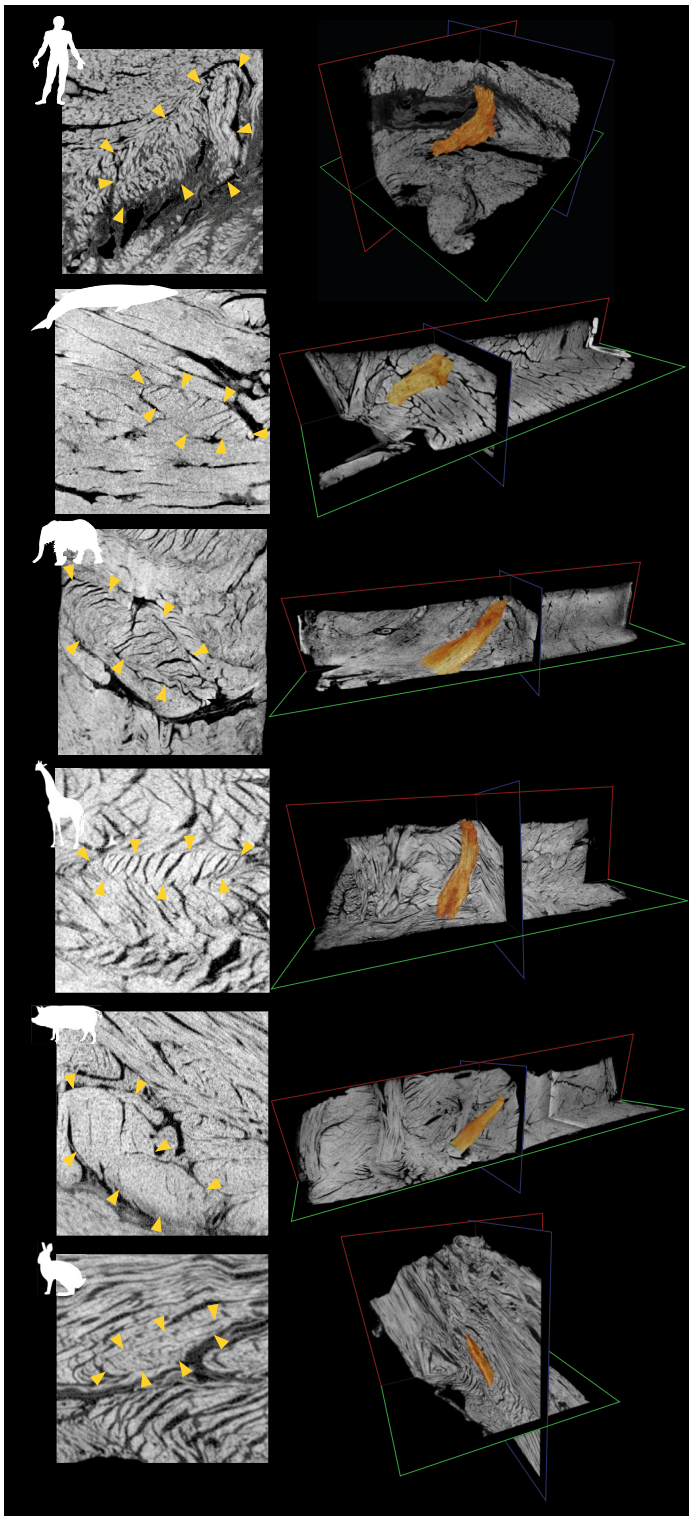

Fig. 9. The panels show how, in all species, aggregation also occurs at a higher order within the three-dimensional mesh to produce bundles, which can be recognised on the basis of their abrupt changes in orientation relative to the surrounding tissue. The bundles can then be traced transmurally. The transitional zones within the overall mesh are outlined with yellow arrows in left panels. The right panels display the three-dimensional transmural extent of the bundles. The segmentation is not based on compartmentalisation, but strictly on the orientation of the aggregated cardiomyocytes.

We make these suggestions based on our observation of the extent of local heterogeneity. In short, the heart has, and requires, subpopulations of myocytes that deviate from the tangential plane to provide antagonism to mural thickening. In this way, it proves possible for the heart to maintain a physiologically desirable shape, and to harness active diastolic forces[29].

The epicardium moves inwards with the same volume as the stroke volume. The wall itself, however, must be squeezed into the decreasing diameters, with a consequent increase in mural thickness. Owing to the branching nature of the myocardial mesh, this "repacking" cannot be achieved by large volumes of the wall moving relative to each other. Instead, it needs to be brought upon by small degrees of slippage between adjacent aggregates. This is achieved along the perimysial clefts. The result is a complicated structure, almost fractal in nature, as depicted in the radial images presented in Fig. 4. Of note, some groups of aggregates, which we have described as bundles, depart from the tangential alignment, adopting a marked angle of intrusion (Fig. 7 and 8). This is particularly obvious in the inner layers, where repacking and slippage is most pronounced. Although the intrusion angle antagonistically erodes some of the circumferential force of the more tangentially orientated cells, it has been presumed to assist with radial repacking[29]. It is also feasible that a tangentially arranged aggregate could be repacked radially within a slippage plane by a connected neighbouring aggregate oriented in transmural fashion, which itself then shortens in a radial direction.

Clinical perspectives

For decades, diffusion tensor imaging studies have been conducted assessing the orientation of myocardial aggregates without prior comprehensive knowledge of their anatomical appearance, which has hindered comprehensive understanding of the results. Diffusion imaging does not allow structures to be assessed based on their anatomical appearance. It is essentially a pseudo-measure based on diffusional properties of the tissue. Convincing results, nonetheless, have been provided showing that changes in the orientation of the aggregates, as assessed with diffusion tensor imaging through the cardiac cycle, are a determinant of cardiac function in both health and disease[6,8], and the clinical availability and the non-invasive nature of the technique make it superior to all other modalities that can quantify the microarchitecture of a tissue. Owing to the lack of anatomical knowledge of the manner of aggregation of the cardiomyocytes, the consequences of the enormous differences in resolution between in-vivo and ex-vivo imaging have hitherto been unclear. Our study now supports the notion that the aggregated entities within the three-dimensional mesh are relatively large. This justifies quantifying their orientation using the low resolution currently provided by clinical imaging, albeit that a direct comparison of different resolutions still needs to be performed. Diffusion tensor imaging thus holds a promising potential in future in-vivo studies of myocardial microarchitecture. Our observations also have relevance for emerging virtual cardiac in-silico models. Recent simulations incorporating laminar organisation have demonstrated how rearrangement of the aggregates can influence ventricular function[32,33]. The pronounced heterogeneity we document indicates that such descriptions are simplifications of a continuous myocardial mesh, a consideration that should inform future modelling efforts.

Limitations

We have analysed only one transmural biopsy from each species. Hence, we cannot comment on either intra-organ or intraspecies variation, both of which possibly exist to some extent. Moreover, the resolution obtained varies between data sets, given the markedly different sizes of the biopsies. Any comparisons need to be placed in this context. Our study confirms, nonetheless, that the myocardium is a complex continuum made up of branching chains of aggregated cardiomyocytes in all species, albeit that we have yet to reconstruct the overall configuration of the mesh across the entire ventricular walls. The continuous nature of the myocardial mesh dictated the need for us to perform subjective, non-automated segmentation of the aggregates, which is subject to human error. Applying our rule-based segmentation method outlined in the methods section, nonetheless, served to yield comparable results across multiple samples, species, and investigators.

Data availability

The data sets analysed during the current study are available from the corresponding author on reasonable request.

Received: 5 March 2025; Accepted: 3 March 2026
Published online: 13 March 2026

References

1. Agger P, Omann C, Laustsen C, Stephenson RS, Anderson RH. Anatomically correct assessment of the orientation of thecardiomyocytes using diffusion tensor imaging. Nmr Biomed. 2019;33:e4205.
2. Lunkenheimer, P. P. et al. What is the clinical significance of ventricular mural antagonism?. *Eur. J. Cardio-thorac.* **53**, 714–723 (2018).
3. Stephenson, R. S. et al. Resolving the true ventricular mural architecture. *J. Cardiovasc. Dev. Dis.* **5**, 34 (2018).
4. Ferreira, P. F. et al. Automating in vivo cardiac diffusion tensor postprocessing with deep learning–based segmentation. *Magn. Reson. Med.* **84**, 2801–2814 (2020).
5. LeGrice, I. J., Takayama, Y. & Covell, J. W. Transverse shear along myocardial cleavage planes provides a mechanism for normal systolic wall thickening. *Circ. Res.* **77**, 182–193 (1995).
6. Nielles-Vallespin, S. et al. Assessment of myocardial microstructural dynamics by in vivo diffusion tensor cardiac magnetic resonance. *J. Am. Coll. Cardiol.* **69**, 661–676 (2017).
7. Agger, P. et al. The myocardial architecture changes in persistent pulmonary hypertension of the newborn in an ovine animal model. *Pediatr. Res.* **79**, 565–574 (2016).

8. Omann, C. et al. Resolving the natural myocardial remodelling brought upon by cardiac contraction; a porcine ex-vivo cardiovascular magnetic resonance study of the left and right ventricle. *J. Cardiov. Magn. Reson.* **21**, 35 (2019).
9. Agger, P. et al. Changes in overall ventricular myocardial architecture in the setting of a porcine animal model of right ventricular dilation. *J. Cardiov. Magn. Reson.* **19**, 93 (2017).
10. Harrington, K. B. et al. Direct measurement of transmural laminar architecture in the anterolateral wall of the ovine left ventricle: New implications for wall thickening mechanics. *Am. J. Physiol. Heart Circ. Physiol.* **288**, H1324–H1330 (2005).
11. LeGrice, I. J. et al. Laminar structure of the heart: Ventricular myocyte arrangement and connective tissue architecture in the dog. *Am. J. Physiol. Heart Circ. Physiol.* **269**, H571–H582 (1995).
12. Legrice, I., Hunter, P., Young, A. & Smaill, B. The architecture of the heart: A databased model. *Philos. Trans. R. Soc. Lond. Ser. Math. Phys. Eng Sci.* **359**, 1217–1232 (2001).
13. Buckberg, G. D., Nanda, N. C., Nguyen, C. & Kocica, M. J. What is the heart? Anatomy, function, pathophysiology, and misconceptions. *J. Cardiovasc. Dev. Dis.* **5**, 33 (2018).
14. Torrent-Guasp, F. Anatomia funcional del corazón : la actividad ventricular diastólica y sistólica. (1957).
15. Agger, P. et al. Insights from echocardiography, magnetic resonance imaging, and microcomputed tomography relative to the mid-myocardial left ventricular echogenic zone. *Echocardiogr* **33**, 1546–1556 (2016).
16. MacIver, D. H. et al. The end of the unique myocardial band: Part I. Anatomical considerations. *Eur. J. Cardiothorac. Surg.* **53**, 112–119 (2018).
17. Wang, S., Cui, J., Jing, Y. & Varray, F. Oscillation of the orientation of cardiomyocyte aggregates in human left ventricle free wall. *J. Anat.* https://doi.org/10.1111/joa.13795 (2022).
18. MacIver, D. H. et al. The end of the unique myocardial band: Part II. clinical and functional considerations. *Eur. J. Cardio-thorac.* **53**, 120–128 (2018).
19. Trainini, J. et al. Evidence that the myocardium is a continuous helical muscle with one insertion. *Rec. Cardioclinics* https://doi.org/10.1016/j.rccl.2022.01.006 (2022).
20. Rodríguez-Padilla, J. et al. Impact of intraventricular septal fiber orientation on cardiac electromechanical function. *Am. J. Physiol. Heart Circ. Physiol.* **322**, H936–H952 (2022).
21. Streeter, D. D. *Gross Morphology and Fiber Geometry of the Heart*. 61–112 (1979).
22. Lunkenheimer, P. P. & Niederer, P. Hierarchy and inhomogeneity in the systematic structure of the mammalian myocardium: Towards a comprehensive view of cardiodynamics. *Technol. Health Care* **20**, 423–434 (2012).
23. Stephenson, R. S. et al. High-resolution contrast-enhanced micro-computed tomography to identify the cardiac conduction system in congenitally malformed hearts valuable insight from a hospital archive. *JACC Cardiovasc. Imaging* **11**, 1706–1712 (2018).
24. Stephenson, R. S. et al. Contrast enhanced micro-computed tomography resolves the 3-dimensional morphology of the cardiac conduction system in mammalian hearts. *PLoS ONE* **7**, e35299 (2012).
25. Anderson, R. H., Smerup, M., Sanchez-Quintana, D., Loukas, M. & Lunkenheimer, P. P. The three-dimensional arrangement of the myocytes in the ventricular walls. *Clin. Anat.* **22**, 64–76 (2009).
26. Garcia-Canadilla, P. et al. Complex congenital heart disease associated with disordered myocardial architecture in a midtrimester human fetus. *Circ. Cardiovasc. Imaging.* **11**, e007753 (2018).
27. Hales, P. W. et al. Histo-anatomical structure of the living isolated rat heart in two contraction states assessed by diffusion tensor MRI. *Prog. Biophys. Mol. Biol.* **110**, 319–330 (2012).
28. Rossi, M. A., Abreu, M. A. & Santoro, L. B. Connective tissue skeleton of the human heart. *Circulation* **97**, 934–935 (1998).
29. Lunkenheimer, P. P. et al. The forces generated within the musculature of the left ventricular wall. *Heart* **90**, 200–207 (2004).
30. Jouk, P.-S., Usson, Y., Michalowicz, G. & Grossi, L. Three-dimensional cartography of the pattern of the myofibres in the second trimester fetal human heart. *Anat. Embryol. (Berl).* **202**, 103–118 (2000).
31. Buckberg, G. D. Echogenic zone in mid-septum: Its structure/function relationship. *Echocardiography* **33**, 1450–1456 (2016).
32. Zheng, Y. et al. Effects of myocardial sheetlet sliding on left ventricular function. *Biomech. Model. Mechanobiol.* **22**, 1313–1332 (2023).
33. Osouli, K., Gaetano, F. D., Costantino, M. L. & Peirlinck, M. Heart in a knot: Unraveling the impact of the nested tori myofiber architecture on ventricular mechanics. *Biomech. Model. Mechanobiol.* **24**, 1815–1835 (2025).

Acknowledgements

The authors would like to thank Prof. Lene Boel at the Department of Forensics, Aarhus University for providing access to the human tissue, Prof. Mads Frost Bertelsen at Zoo Copenhagen for providing access to elephant tissue, and Ree Park, Ebeltoft, for providing access to giraffe tissue.

Author contributions

RS designed the study, scanned the specimens, performed the segmentation and data analyses, and drafted the initial manuscript. JP reviewed and edited the manuscript and provided important insights on functional interpretation. JJ reviewed and edited the manuscript. RM and SH performed the high-resolution scans on the human, rabbit, and porcine tissue. RHA reviewed and edited the manuscript and provided insights on myocardial morphology. PA designed the study, gathered and provided the tissue, performed the data analyses, drafted the initial manuscript, and edited and submitted the final manuscript.

Funding

PA is supported by the Lundbeck Foundation, the Danish Children Heart Foundation, and the Riisfort Foundation.

Declarations

Ethical declarations

All methods were carried out in accordance with relevant guidelines and regulations. All animal tissue was obtained from animals that either died of natural causes or were euthanised due to disease or as part of breeding programs. Thus, no animals were killed for the sole purpose of this study. All animal specimens have been collected in accordance with Regulation No. 1069/2009 of the European Parliament (The animal by-product Regulation). The human tissue was scanned as a part of a forensic autopsy. The handling of the tissue strictly followed the Danish legislation that applies to a forensic autopsy including procedures on anonymisation and data handling.

Competing interests
The authors declare no competing interests.

Additional information
Supplementary Information The online version contains supplementary material available at https://doi.org/10.1038/s41598-026-43337-7.

Correspondence and requests for materials should be addressed to P.A.

Reprints and permissions information is available at www.nature.com/reprints.

Publisher's note Springer Nature remains neutral with regard to jurisdictional claims in published maps and institutional affiliations.